Group project for the course of

Mechanical Design for Mechatronics

Prof.: Rustighi Emiliano

Technical report

Design of the Structure of an Automated Machine for Agricultural Purposes

---

Bontempelli Elia
Rizzardi Alessandro

Dalle Vedove Matteo
Zambotti Beatrice

August 19, 2022

Contents

1 Product design specification

The goal of our project is to create our implementation of the *CyberOrto* [**cyberorto**] made by *Mindshub*, a non-lucrative association based in Ala (Trentino). The goal of this robot is to automatically handle an amateur vegetable garden by performing this 3 principle actions:

i) planting the seeds of the desired plant in a location decided by the user using a web interface;

ii) constantly provide water to the vegetable;

iii) extirpate undesired plants.

By talking with the association that worked (and is still improving) on the product we acknowledged the following requirements (mainly related to the functionality of the product) that the machine has to satisfy:

i) the arm appendix must suits an interface that allows to have an interchangeable set of tools (like the one use to plow the terrain);

ii) the arm appendix should accommodate a small pipe in order to irrigate the vegetables; in particular this has to be connected to an external reservoir (with no dimension specified if it's position is fixed) or by using an internal reservoir on the moving structure of at least $4l$ (that can periodically be refilled) if it's not possible to directly attach the arm to the main reservoir;

iii) the minimum accepted working area of the robot is a rectangle of dimension $4m \times 3m$; the robot should be design keeping in mind the possibility to increase the working area by expanding it over one edge (for example having the possibility to work on a $8m \times 3m$ terrain);

iv) the structure can house the electronic control unit of the robot that's remotely connected to the server using wireless connection and by doing so should accommodate a battery the allows the robot to work for at least $4h$. The power consumption of the structure should be minimized if possible (at the actual state the prototype consumes $40W$ and has a battery of $240Wh$ weighting $6.3kg$);

v) regarding the accuracy of the movement of the system the allowed backlash on the working point should always be less then $1cm$ with the control technique implemented and the goal is to have maximum $5mm$ of deviation from the nominal value;

vi) the structure should be mainly composed of standard components and should be as cheap as possible in order to make it affordable for everyone.

Loads and operating conditions   The structure should be able to perform all it's operation while being safe and fully functional. For the design and the verification of the structure the loads related to wind can be neglected due to the presence of an anemometer that's mounted on the robot that's ensuring that the robot works only on a sufficiently safe environment.

The heavier operation performed by the robot is the extirpation that's done by plowing the soil with a rotating element **AGGIUNGERE UNA BREVE DESCRIZIONE**. Considering the actual mounted motor to perform this operation the torque that has to be transmitted to the plower is of $T_{\text{plower}} = 0.8N \cdot m$.

1.1 Requirements & specifications

With this promise being said, it's possible to express the main requirements, associated to the aim dictated by our customer and our design rules, and the specifications of the designed machine. All this information, collected in table 1, has to be considered in each step of the design phase in order to develop the mechanical solution.

While developing the project other factors should be kept in mind:

- the possibility to pack all the necessary components in a *small* transportation box (the box shouldn't present and edge greater than $2m$, maximum sum of all the edges less then $3m$) in order to avoid shipping issues;

- the kit should be feasible to all private enthusiast that enjoy *do-it-yourself* projects and this has to kept in mind; the final assembly should be made possible by common mounting tools (such screwdrivers, Allen keys...) that can be easily purchased and used by the customer; for the same reason welding finishes are not recommended.

1.2 Goal of our project

Designing the whole machine is out of our scopes as it is very complex and requires knowledge that we still miss, so we decided to focus our work in the design of the main structure of the robot putting effort in the structural verification as the goal of the course.

2 Concept generation

With all the premise that lead the development of the project, the first thing that has to be done is generate the concept that can later be compared to choose the best design solution that can become a concrete realization of the ideas.

Kinematic configurations The first key operation that the robot has to perform is reaching a desired point on the working space and so, in planar kinematics, the machine should present two degrees of freedom that allow to reach all the possible positions; this can be done considering 3 main joint configuration that allows to perform such operations:

- double prismatic joints (figure 1.a) where two perpendicular linear guides can be used to move on the plane;

- prismatic and revolute joint (figure 1.b) where the arm that's free to rotate it's mounted on top of a linear guide. This kind of kinematic chain is currently used by the MindsHub concept;

Table 1: full list of requirements and specifications for the CyberOrto project.

1) Geometry:

    1.1) dimension of the terrain to cultive — at least $4m \times 3m$, extendible if possible

    1.2) vertical clearance from the ground of the robot while moving — $\geq 50cm$

2) Kinematic:

    2.1) time travel between further points in the field — $\leq 10s$

    2.2) accuracy of the working appendix respect to nominal value — max $\pm 1cm$, target $\pm 5mm$

3) Energy:

    3.1) low energy consumption — max 40W, target 20W

    3.2) in-device battery with docking station — battery $\geq 240Wh$ or 4+ hour of work

4) Functionalities:

    4.1a) provide direct water access to irrigate the soil

    4.1b) or provide a reservoir that can be automatically refilled on a docking station — $\geq 4l$

    4.2) standard mount on the appendix arm that can fit multiple working tools

    4.3) plowing the terrain — $T_{\text{plower,max}} = 0.8N \cdot m$

    4.4) provide a pneumatic circuit used for the appendix that plants seeds

5) Materials:

    5.1) components standardization — very high

    5.2) materials should be weather proof (oxidation free)

6) Terms of use:

    6.1) easy to assemble — max 2 persons required

    6.2) fatigue resistance — infinite life-cycles if possible, min 10^6

    6.3) insensible to environmental conditions (weather and dirt)

7) Loading conditions:

    7.1) wind and environmental actions can be neglected with robot in action

8) Costs: — $\leq €2\,000$

- double revolute joints (figure 1.c), typical configuration of a robot arm, that constraint the framing point to be fixed.
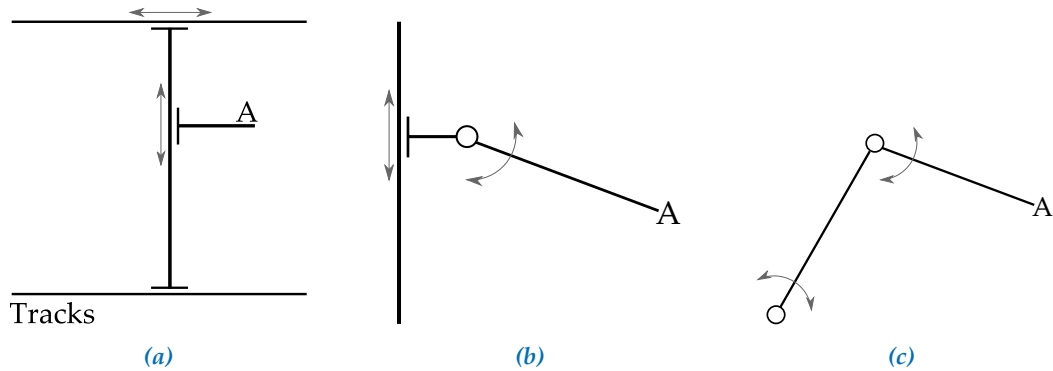
(a)   *(b)*   *(c)*

Figure 1: main kinematics coupling that allows to univocally determine the position of a point A in a plane: (a) double prismatic joints, (b) prismatic and revolute joint, (c) double revolute joints.

By a first analysis the third configuration (double revolute joint) isn't feasible for the project due to the fact that the system presents a fixed pivot point respect to the frame and to work more area it's mandatory to increase the length of the edges (and this is an issue for the *extendibility* of the machine).

Concept #1   The first concept (figure 2) is realised with a double prismatic joint. In particular point A and A' lies on parallel tracks placed on the ground that can be extended in order to increase the cultivated area. The working arm can move along an elevated beam connecting the track (point B) and can move vertically to cultivate point P.
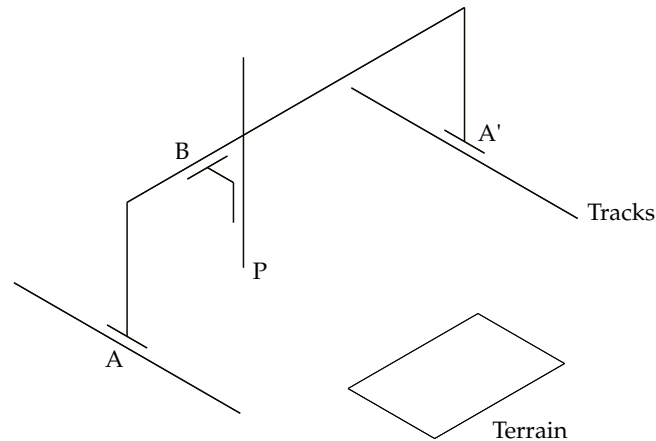

Figure 2: concept #1 realised with double prismatic joint.

This structure present a frame for the arm that's stable while operating due to it's arch structure; possible problem to this implementation is that long elevated beam (subjected to the loads of the arms and it's mass) can deflect and fail statically. Also, if possible, rotoidal coupling should be used (and for this we can refer to concept #2).

4

Concept #2 The second concept (figure 3) is similar to the first one but one prismatic joint is replaced with a revolute connection put in the middle of the elevated beam. The length of the edge *BP* from a top view must be equal to half the length of the supporting bar in order to reach all points in the rectangular space.
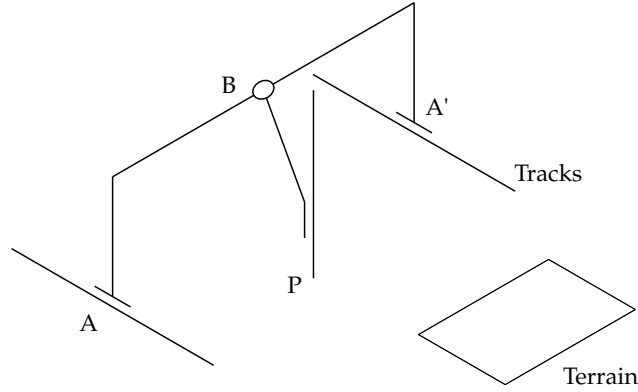

Figure 3: concept #2 realised with a combination of both prismatic and revolute joint.

This structure also presents the pro of concept #1 of having a stable frame structure for the operating arm due to it's arch conformation and, as addition, uses a revolute joint to control the second degree of freedom of the arm. However this implementation increases the mechanical load on the elevated beam (increasing the torsion due to the higher arm of the actions on the tool tip respect to the elevated bar).

Concept #3 The third concept (figure 4) is similar to #2 but instead of using two parallel tracks, the prismatic joint uses only one of them.
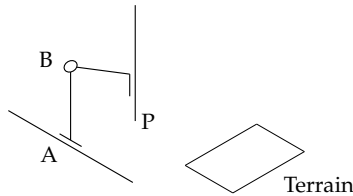

Figure 4: concept #3 realised with a combination of both prismatic and revolute joint.

This implementation avoid the problem of high deflection of concepts #1 and #2 by removing the long elevated framing beam, but also increases the reactional momentum that the prismatic joint *A* should bear in order to maintain stable the system.

2.1 Decision matrix

With a brief overview of the 3 main concept generated, the unbiased choice can be performed by constructing and evaluating the decision matrix (table 2). The main objective evaluated are:

- costs: based on the estimated material cost considering quantity and types of parts that can be used for the implementation;

- reliability: expected mechanical resistance of the structure subjected to nominal loads as well as unexpected external loads (such environment of customer that interact with the structure);

Table 2: *decision matrix.*

Objective	Weight	Parameter	Concept #1			Concept #2			Concept #3		
			Mag	Score	Value	Mag	Score	Value	Mag	Score	Value
Material costs	0.2	relative €	medium	7	1.4	high	5	1	low	9	1.8
Reliability	0.3	experience	good	8	2.4	okay	6	1.8	poor-fair	3	0.9
Lifetime	0.15	experience	great	10	1.5	good	8	1.2	fair	4	0.6
Adaptability	0.2	experience	good	8	1.6	okay-good	7	1.4	fair	4	0.8
Team experience	0.15	experience	good	8	1.2	great	10	1.5	fair	4	0.6
Overall score:					**8.1**			6.9			4.7

Qualitative score assignments: poor = 2, fair = 4, okay = 6, good = 8, great = 10.

- lifetime: expected lifetime of the product based on fatigue considerations;

- adaptability: criteria that evaluates how easy is to modify geometrical parameters to meet specific custom requirement of the final customer based on asperity and tolerances of the terrain to cultivate;

- team experience: based on the overall design feasibility made by the team.

With the decision matrix completed the chosen concept is the first on which the motion is performed only by prismatic joints.

2.2 Material selection

The main structural components are beams that, for client requirements, should be standard and so for this reason T slot extruded aluminium profiles (figure 5) are chosen after the following considerations:

- better volume-to-price ratio and lower density (respect to inox steels), so reducing costs associated to the spare parts and shipping;

- availability in the market: there are a lot of vendors that provide profiles with various geometrical dimensions, different aluminium alloy and surface finishes. This spare parts can be easily accessed by every private costumer;

- for T slot extruded profiles lots of auxiliary components (such supporting brackets, fasteners, hinges...) are provided from the same profiles manufacturers, reducing the need of custom made part and so decreasing the overall costs.

This elements can be also purchased with an anodized finish that allows to improve the corrosion resistance, increasing so the expected life time of the product in uncontrolled outdoor environment.
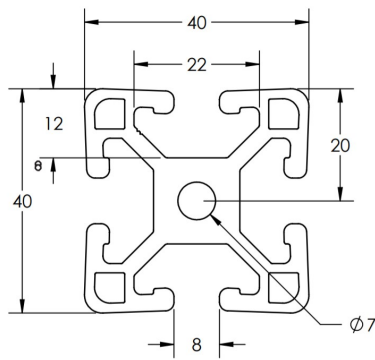

*Figure 5: technical drawing of a T-slot profile's cross-section. The particular sketch represent the model TS40-40LM by Tslots [**tslot-ds**].*

Mechanical properties   For the design part the following mechanical properties are considered: ultimate tensile strength $\sigma_{uts} = 260 MPa$, yielding strength $\sigma_{ys} = 240 MPa$, Young's module $E = 70 GPa$, Poisson's ratio $\nu = 0.32$; this values are chosen according to table A.1.1 (page 21) as they represent a lower bound (implying higher safety in calculations) for the aluminium material used for the T-Slot sections.

3 Preliminary design

Based on the selected concept the simplest body diagram has been created in order to start the dimensioning of the main elements of the structure. Considering the possible practical implementation of the system, the symbolic representation of the moving frame has been made (figure 6).
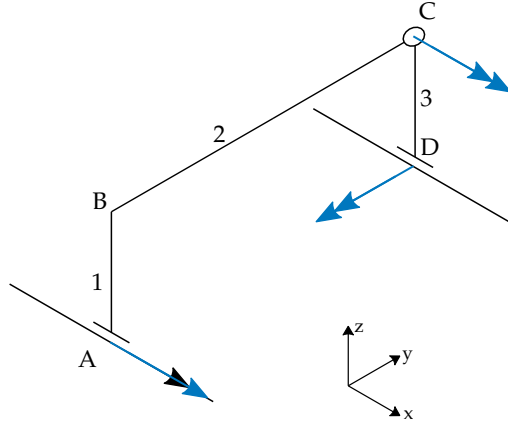

Figure 6: *schematic representation of the moving frame supporting the arm; blue arrows are describes the rotational degree of freedom left by the joints.* **FIGURA DA MODIFICARE**

The design involves a main elevated track (body 2) supported by two vertical supporting beams (bodies 1 and 3); the connection between body 1 and 2 is constituted by a full joint in point B constraining all 6 degrees of freedom while the connection of the track with the other support is done by a hinge that leaves free the rotation over the global x axis. The two vertical supports can slide on two parallel tracks and the associated prismatic joints constraints respectively 5 and 4 degrees of freedom in A and D, leaving the system free to slide along the x global axis; the choice of leaving also D in as free to rotate aims at reducing redundant constraints, with the aim of reducing hyperstatic variables with a design that accommodates misalignments in the position of the two parallel tracks placed at ground.

As simplification on both the geometry and the load we consider:

- on the elevated track the loads transferred by the working appendix are modelled as a pure vertical force F (mainly related to the approximate weight of the turret that contains all equipment) and a torque T that model's the one due to the plower; the eccentricities of both forces are in this case neglected and the application of application of both actions is placed at a distance ζ referred to the local coordinate z of the elevated track, figure 7*(b)*;

- the vertical supports are equally dimensioned and present a characteristic height $H = 700mm$; the elevated track connecting them has length $L = 3000mm$ as dictated by the customer requirements;

- figure 7*(a)* shows the free body diagram of the structure and thus the set of external actions and reactions applied; figure 7*(b)* reports instead the reference frames with respective origin with respect to which internal loads are calculated.
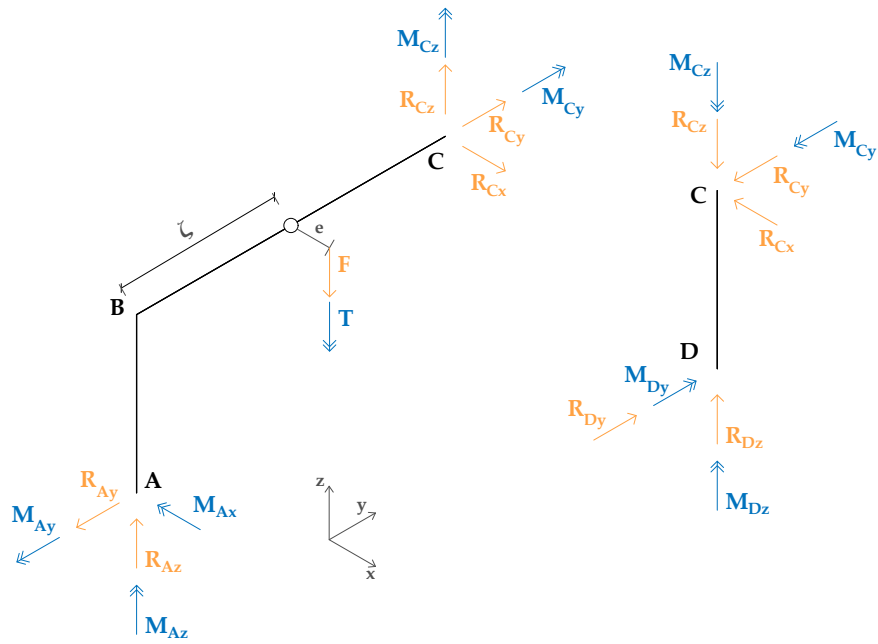
(a)
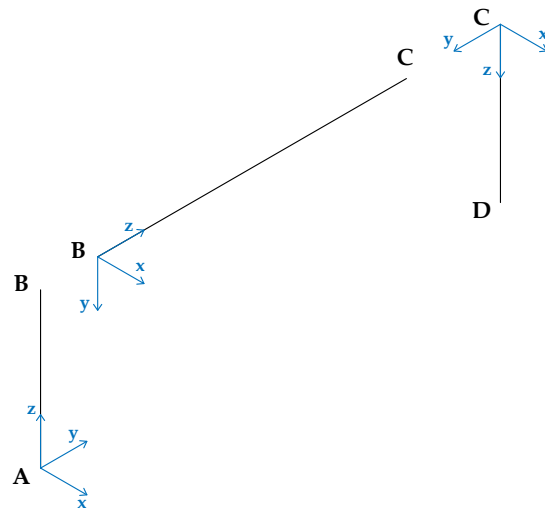
(b)

Figure 7: *free body diagram (a) and reference frames (b) used for the description of the internal loads of the beam. In (a) the structure has been disassembled at the pivot point C in order to describe the reaction forces transmitted.*

The full joint in B has not been described (as the connection preserves the continuity of the actions transmitted by the body), however the final design will imply the connection of two separate beams by means of a gusset.

After having written the Newton-Euler equations of the two bodies making the whole structure, we observe that only 11 out of 14 reactions forces are independent; chosen the hyperstatic variables $X_1 = M_{Az}, X_2 = M_{Dy}, X_3 = M_{Ax}$ to reduce the problem to an isostatic one, the parametric definitions of the reaction forces is

$$R_{Az} = \frac{F(L - \zeta) - X_3}{L} \qquad R_{Cz} = R_{Dz} = \frac{F\zeta + X_3}{L}$$

$$M_{Ay} = M_{Cy} = X_2 \qquad M_{Cz} = M_{Dz} = T - X_1$$

Non mentioned actions are identically zero. To solve the hyper-static problem the Castigliano's theorem has been used, computing the elastic energy U_e of the structure neglecting shear loads:

$$U_e = \sum_{i=1}^{3} \int_0^{l_i} \left(\frac{N_i^2}{2EA_i} + \frac{M_{x,i}^2}{2EI_{xx,i}} + \frac{M_{y,i}^2}{2EI_{yy,i}} + \frac{M_{z,i}^2}{2GJ_{t,i}} \right) dz$$

Assuming the generalized displacement related to the hyper-static variables is zero, solving the equations $\partial U_e / \partial X_1 = 0$ and $\partial U_e / \partial X_2$, the solution that we achieve is still depending on the geometrical parameters of the sections that are still unknown. To simplify the calculations, assuming that A_1 gives

$$X_1 = T \qquad X_2 = 0 \qquad X_3 = F\frac{L - 2\zeta}{2}$$

In this preliminary design phase in order to over-estimate the loads the the frame should bear a force $F = 200N$ is considered (modelling the weight of about $20kg$, related to all the carried equipment on the moving arm including batteries and filled water tank) and the nominal value of the torque $T = 0.8N \cdot m$ as in the requirements specification.

Choice of the standard beams With the preliminary design model described, different solutions can be found looking from various vendors present in the marker. In particular for the project main reference has been made to the Parker IPS catalogue [**parker-ds**] due to the high availability of accessories components, however similar product can be found by other vendors (as group we also evaluated 8020 [**8020-ds**] and Tslots by Bonnel Aluminum [**tslot-ds**]).

Data-sheets presents information about the section area A and second moments of area I_{xx}, I_{yy} respect the primary axes, however no information is given for the torsional rigidity J_t and so the related component is in the calculation neglected.

After an iterative process, table 3 shows the sections drawing and associated geometric properties of the chosen components for both elevated track and supporting beams. This choice determines a safety factor $\phi = 3.8$ for the whole structure that's a safe value for us; it is true that we neglected both shear and torque loads, and in practical applications other external and unexpected actions might act on the frame, however it is also true that the geometric simplification A_1 in the solution of the hyperstatic problem heavily reduced the ability of the system to bear load (as we will see in the static verification).

Usage	Area $A[cm^2]$	Moments of inertia $I_{xx}[cm^4]$	$I_{yy}[cm^4]$	Weight $\rho[kg/m]$	Product code
track	6.65	9.46	9.46	1.72	10-040
supports	5.20	8.27	8.27	1.41	10-540
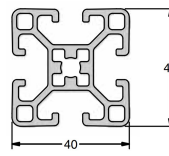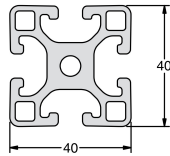
Sections for the track beam (on the left) and the supports (right).

As a side note, our design was forced to use the 40*mm* T-slot series (even if a 30*mm* profile would have let us achieve similar results with lower weights and costs) as it's the only one that disposes off-the-shelf linear roller system that can be easily mounted and used (choosing other profile series would have ended in custom solution that's undesired by the product design specifications).

4   Design process and verifications

With the data obtained from the preliminary analysis, the design has been carried using the 3D CAD software `AutoDesk Inventor Professional` with the help of the components library provided by the manufacturer Parker IPS. At this stage what we mainly did was to *give shape* at the chosen concept by using mechanical elements provided by the library only in order to minimize the need of custom-made parts.

For actuating the machine no off-the-shelf solution are available, hence we decided to create our custom rack design (**INSERIRE E CREARE RIFERIMENTO AL DISEGNO**): such component is made by a set of smaller bid that can be 3D printed with plastic material; such elements can be joined together by means of standard T-slot components. The rack is mounted on both tracks placed at the ground (motion in the x direction) and the elevated one (motion in the y direction); the gear attached to the motor that's actuating the system is a standard element made out of steel. Proper static verification of the component will be described in the following pages.

Using the theory from the course we performed a static verification of the machine and we verified two critical bolted joints.

4.1 Static verification

With all the geometrical values known, it has been possible to carry out a more detailed analysis. Considering a more complex model of the forces that takes into account also the distributed load due to the gravity and that the force F is applied with an eccentricity $e = 5cm$, it has been possible to parametrically define the hyperstatic variables as

$$X_1 \simeq \left(0.63 - 0.16\zeta\right)N \cdot m \qquad X_2 \simeq -8.10 \ N \cdot m$$

$$X_3 \simeq \left(-10.54 - 11.07\zeta + 55.53\zeta^2 - 6.17\zeta^3\right)N \cdot m$$

Evaluating the stress state on the 3 beams making up the structure for values of $\zeta \in [0, L]$, what we obtained is that the most critical section is in the elevated track for $\zeta^* = 1.65m$ at $z^* = 1.65m$ where the maximum bending value $M_x^* \simeq 135.64N \cdot m$ is achieved. Knowing that $N^* = 0$ and neglecting the shear stress contribution due to both shear $V_y^* \simeq 111N$ and torque $M_z^* \simeq 1.89N \cdot m$, the stress state is

$$\sigma_{zz}(y) = \frac{M_x^*}{I_{xx,track}}y \qquad \Rightarrow \qquad \sigma_{zz,max} = \sigma_{zz}(2cm) \simeq 28.68MPa$$

This leads to a safety factor of $\phi = \sigma_{ys}/\sigma_{zz,max} \simeq 8.37$, meaning that the structure is statically verified. This value is more then twice than the one achieved in the preliminary design phase but is due to the fact that in this case the full analytical solution of the hyperstatic problem has been considered, having determined all geometrical properties of the sections. As a reminder:

- due to the lack of analytical formulas for such complex geometry section, shear components due to torque and shears are neglected and could have influenced the mechanical system;

- we did not consider external forces acting that might act on the global x axis due to the actuation of the machine or accidental load applied by the end user: this can lead to an increase in bending and torques that might make the system fail.

MAGARI AGGIUNGERE GRAFICI DEL MOMENTO IN FUNZIONE DI 2/3 VALORI DI ζ
AGGIUNGERE LA STIFFNESS VERIFICATION

4.2 Fatigue verification

Most critical section As already stated, the most critical section is subjected to a maximum stress of $\sigma_{max} \simeq 28.68MPa$. While functioning we expect that the turret performing the operation to the soil periodically moves along the track: having ζ varying over time determines that also the internal loads are fluctuating and this might arise fatigue failure of the machine.

Given the need of a fatigue verification, acknowledged that the minimum bending load at z^* is $M_{x,min} \simeq 14.05N \cdot m$ achieved for $\zeta = 0m$, determining $\sigma_{min} \simeq 2.97MPa$; this further implies that the mean and amplitude stresses for fatigue verification are

$$\sigma_m \simeq 15.82MPa \qquad \sigma_a \simeq 12.85MPa$$

According to Soderberg criterion, the equivalent amplitude only stress component evaluates to

$$\sigma_{a,eq} = \frac{\sigma_{ys}\sigma_a}{\sigma_{ys} - \sigma_m} \simeq 13.76 MPa$$

In this case the load factor is $C_l = 1$; given an equivalent diameter $d_{eq} = \sqrt{\frac{4}{\pi}A} = 29mm$, the corresponding size factor is $C_d = 1.189 d_{eq}^{-0.097} \simeq 0.86$; details concerning the surface finish of the T-slot beams are not enough to fully determine the surface coefficient C_s that's assumed in this case to be 0.8 as safety value. Considering an endurance limit of the 6061-T5 aluminium alloy of $\sigma_{lim} = 100 MPa$ [**aluminium-endurance**], this means that the safety factor against fatigue failure is

$$\phi_{\text{fatigue}} = C_s C_d C_l \frac{\sigma_{lim}}{\sigma_{a,eq}} \simeq 4.98$$

4.3 Threaded joints verification

Preliminary design

Given the customer's requirements, the threaded fasteners used for the threaded joints in the whole robot are chosen to be standard screws with diameter of $8mm$, compatible with the $40mm$ T-slot profiles.

Considering the threaded joints present on the robot, the maximum thickness of the members is given by the sum between the beam cross section's width, $40mm$, and the machined gussets thickness, $8mm$. Given that two screws must fit, as in section A, the length of the screws is chosen to be equal to $18mm$, according to `UNI ISO 888`; table 4 reports main properties of the chosen bolt used for the verification of the connections.

*Table 4: selected bolt chosen from the Parker IPS catalogue [**parker-ds**] and related main properties.*

Parameter	symbol	value
diameter	d	$8mm$
head diameter	d_0	$14mm$
length	l	$18mm$
cross-section	A_b	$16\pi mm^2$
tensile cross-section	A_{bt}	$36.6mm^2$
ultimate tensile strength	σ_{uts}	$505MPa$
product code		24-118-8

With reference to Figure 6, threaded joints are present in sections A, B, C and D. The verifications are carried out with respect to the most critical sections which, according to the load analysis performed previously, are identified as section A and D. Moreover, since the load distribution depends on the position of the point of application of the external load, the most critical condition corresponds to the one in which the load is applied in $\zeta = 1$ for section A and $\zeta = 3$ for section D.

Section A

The loads applied on section A are the following:

- axial load $N_A = -251.126N$;

- bending moment $M_{xA} = -12.645N \cdot m$;

- bending moment $M_{yA} = 1.894N \cdot m$;

- torque $M_{zA} = -0.594N \cdot m$.

In correspondence of section A, there are two machined gussets chosen from the Parker IPS catalogue [**parker-ds**], reported in figure 8. Given the geometry of the component, the threaded joints are positioned on the vertical z and horizontal x global axis. For this reason, two separated analysis are performed.
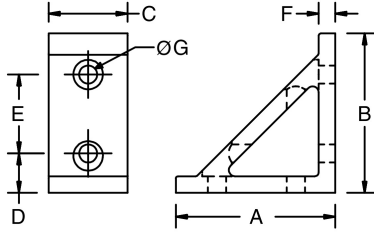

*Figure 8: machined gusset, code 10-102, from the IPS catalogue [**parker-ds**]. In the drawing: $A = 77mm$, $B = 77mm$, $C = 34mm$, $D = 20mm$, $E = 40mm$, $F = 8mm$, $G = 9mm$.*

Threaded joints along the x axis The sliding actions are given by the torque M_{zA}, which produces a shear force on every screw equal to:

$$V_i = \frac{M_{z1}r_i}{\sum\limits_{i=1}^{n_b} r_i^2}$$

where r_i are the distances of every screw from the center of the section O, and are equal to $r_1 = 40mm$, $r_2 = 80mm$. The shear force is calculated for the most critical screws, distant r_2 from O, and it is equal to:

$$V_2 = \frac{M_{zA}r_2}{2r_1^2 + 2r_2^2} = -2.970N$$

The shear and punching resistance verifications can be performed as follow:

- shear resistance verification:
$$|V_2| < \frac{\sigma_{uts}A_b}{\phi}$$

where σ_{uts} corresponds to the screw's ultimate tensile strength, A_b to the bolt cross-section and ϕ is the safety factor which, according to Eurocode3, is equal to $\frac{1.25}{0.58}$. As a consequence, it follows that:

$$\sigma_{uts} > \frac{|V_2|\phi}{A_b} = 0.127MPa.$$

- crushing resistance verification:

$$|V_2| < \frac{\sigma_{uts,m} d t}{\phi}$$

where $\sigma_{uts,m}$ corresponds to the member's ultimate tensile strength, d to the bolt diameter and ϕ is the safety factor which, according to Eurocode3, is equal to 0.5. Finally, t corresponds to the member's thickness, which can be calculated as the sum of the machined gusset thickness, $F = 8mm$, and the base's thickness, equal to $16mm$:

$$\sigma_{uts,m} > \frac{|V_2|\phi}{dt} = 7.734 \cdot 10^{-3} MPa.$$

Separating actions are given by the axial load and the bending moments.
Assuming that the members are rigid it is possible to calculate the effects of the separating actions in both xz and yz planes.
The load caused by the separating action, acting on each bolt can be calculated as:

$$N_i = \frac{M_b h_i}{\sum\limits_{i=1}^{n_b} h_i^2} + \frac{N}{n_b}$$

Considering the xz plane and assuming the pivot is placed on the edge of the section, the constant h_i will be equal to:

$$\begin{cases} h_1 = 16.962mm \\ h_2 = 56.962mm \\ h_3 = 136.962mm \\ h_4 = 176.962mm \end{cases}$$

The normal load is calculated for the most critical screw as follow:

$$N_{xz} = \frac{M_{yA} h_4}{h_1^2 + h_2^2 + h_3^2 + h_4^2} + \frac{N_1}{n_b} = -56.530N$$

Since the axial load acting on every bolt is negative, i.e. the bolt are subjected to compression, there are no issues relative to tension and punching resistance. As a consequence, it is not necessary to perform those verifications. **(???)**

Considering the yz plane and assuming that the pivot is placed on the edge of the section, the constants h_i will be all equal to $\frac{C}{2} = 17mm$. The normal load is equal to:

$$N_{yz} = \frac{M_{xA} h_4}{h_1^2 + h_2^2 + h_3^2 + h_4^2} + \frac{N_1}{n_b} = 123.175N$$

The tension resistance and punching verification can be performed as follow:

- tension resistance verification:

$$N_{xz} < \frac{\sigma_{uts} A_{bt}}{\phi}$$

Where σ_{uts} corresponds to the screw's ultimate tensile strength, A_{bt} to the bolt tensile cross-section and ϕ is the safety factor which, according to Eurocode3, is equal to $\frac{1.25}{0.9}$. As a consequence, it follows that:

$$\sigma_{uts} > \frac{N_{xz}\phi}{A_{bt}} = 4.674 MPa.$$

15

- punching resistance verification:

$$N_{xz} < \frac{\pi d_0 t \sigma_{uts,m}}{\phi}$$

Where $\sigma_{uts,m}$ corresponds to the member's ultimate tensile strength, d_0 the bolt head diameter and ϕ is the safety factor which, according to Eurocode3, is equal to $\frac{1.25}{0.6}$. Finally, t corresponds to the member's thickness, which can be calculated as the sum of the gusset's thickness, $F = 8mm$, and the base's thickness, equal to $16mm$:

$$\sigma_{uts,m} > \frac{N_{xz}\phi}{\pi d_0 t} = 0.243 MPa.$$

Threaded joints along the z axis   In this case the sliding actions are givenc by M_{xA} which produces a shear force on every screw equal to:

$$V_i = \frac{M_{xA} r_i}{\sum\limits_{i=1}^{n_b} r_i^2}$$

where r_i are the distances of every screw from the center of the section O, and are equal to $r = \frac{E}{2} = 20mm$.

$$V = \frac{M_{xA} r}{2r^2} = 14.849N$$

- shear resistance verification:

$$\sigma_{uts} > \frac{V\phi}{A_b} = 0.637 MPa.$$

- crushing resistance verification:

$$\sigma_{uts,m} > \frac{V\phi}{dt} = 3.867 \cdot 10^{-3} MPa.$$

The separating actions, N_A, M_{yA} and M_{zA}, generates axial loads of compression ands, similarly to the x axis case, the verifications are not needed. The calculations are not reported for the purpose of brevity.

Section D

The loads applied on section D are the following:

- axial load $N_D = 233.010N$;

- bending moment $M_{xD} = 0N \cdot m$;

- bending moment $M_{yD} = 8.106N \cdot m$;

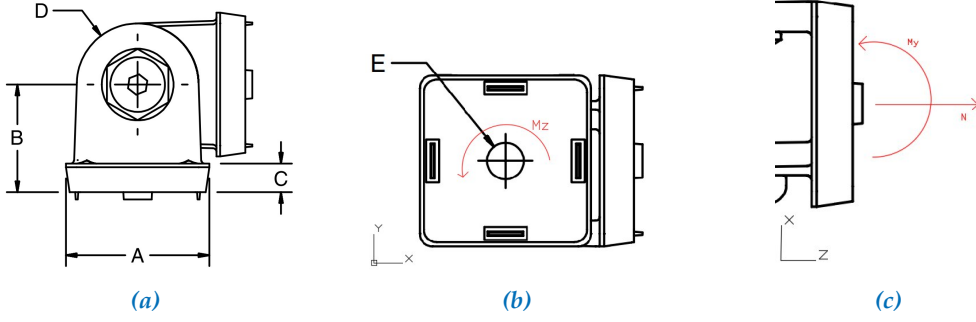- torque $M_{zD}x = -0.594N \cdot m$.

Figure 9: *pivot joint, code* `23-010`*, from the IPS catalogue* [**parker-ds**]*. In the drawing:* $A = 40mm$, $B = 30mm$, $C = 9mm$, $D = 40mm$, $E = 8.5mm$, $F = 60mm$.

In correspondence of section D, there is a pivot joint chosen from the Parker IPS catalogue [**parker-ds**], reported in figure 9.

In this case, the sliding actions are given by the torque M_{zD}, figure 9(b). However, since there is a single screw positioned in the center of the section, they do not cause any shear on the screw. **(??)**

Separating actions are given by the axial load and the bending moments. Assuming that the members are rigid it is possible to calculate the effects of the separating actions in both xz and yz planes. The load caused by the separating action, acting on the screw can be calculated as:

$$N_i = \frac{M_b h_i}{\sum\limits_{i=1}^{n_b} h_i^2} + \frac{N}{n_b}$$

where h_i is the distance of the i-th bolt from the pivot point.

$$N_{xz} = \frac{M_{yD}}{h} + N_D = 638.328N$$

Considering the xz plane and assuming the pivot on the edge of the section, h is equal to $\frac{A}{2} = 20mm$. The tension resistance and punching verification can be performed as follow:

- tension resistance verification:

$$N_{xz} < \frac{\sigma_{uts} A_{bt}}{\phi}$$

Where σ_{uts} corresponds to the screw's ultimate tensile strength, A_{bt} to the bolt tensile cross-section and ϕ is the safety factor which, according to Eurocode3, is equal to $\frac{1.25}{0.9}$. As a consequence, it follows that:

$$\sigma_{uts} > \frac{N_{xz}\phi}{A_{bt}} = 24.223 MPa.$$

- punching resistance verification:

$$N_{xz} < \frac{\pi d_0 t \sigma_{uts,m}}{\phi}$$

17

Where $\sigma_{uts,m}$ corresponds to the member's ultimate tensile strength, d_0 the bolt head diameter and ϕ is the safety factor which, according to Eurocode3, is equal to $\frac{1.25}{0.6}$. Finally, t corresponds to the member's thickness, which can be calculated as the sum of the pivot joint thickness, $C = 9mm$, and the member's cross section, equal to $40mm$:

$$\sigma_{uts,m} > \frac{N_{xz}\phi}{\pi d_0 t} = 0.617 MPa.$$

Considering instead the xz plane we have:

$$N_{yz} = \frac{M_{xD}}{h} + N_D = 233.010 N$$

thus:

- tension resistance verification:

$$N_{yz} < \frac{\sigma_{uts} A_{bt}}{\phi} \qquad \Rightarrow \sigma_{uts} > \frac{N_{yz}\phi}{A_{bt}} = 8.842 MPa.$$

- punching resistance verification

$$N_{yz} < \frac{\pi d_0 t \sigma_{uts,m}}{\phi} \qquad \Rightarrow \qquad \sigma_{uts,m} > \frac{N_{yz}\phi}{\pi d_0 t} = 0.225 MPa.$$

In conclusion, the bolt ultimate strength must be greater than $24.223 MPa$, a value that allows to choose any bolt property class. In order to minimize the costs, property 4.6 is chosen.**(????)**

Moreover, the verifications for crushing and punching provide the minimum member ultimate strength, $\sigma_{uts,m} > 0.226 MPa$, value much smaller than the chosen member's UTS.

Note that for the verifications of the separating actions the rigid member approach was used, which is usually more conservative than the others. However, since the values obtained are far distant from the one of the selected materials, there is no need of a more precise verification.

5 Static verification rack and gear

The verification continued with the parts responsible for actuating the machine, rack that is positioned on both tracks and gear attached on the motors' shaft.
We focused on two important aspects, interference and tooth root bending resistance.

5.1 Interference condition

It's fundamental to check if this condition is fulfilled, because otherwise we could have a problem of undercut, when the tip of the rack cutter is moved beyond the base circle of the gear and the result is the weakening of the gear's teeth.
Interference condition is function of the minimum number of teeth of the pinion, in accordance with the following equation:

$$z_{min} = \frac{2}{\sin^2\alpha}, \tag{1}$$

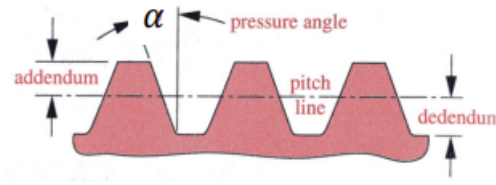where α is the pressure angle, as we can see in Figure 10.

Figure 10: Standard rack

In our case we have:
$$\alpha = 20 \Rightarrow z_{min} = 17,$$

that means that the interfence condition, in our project, is fulfilled because we designed a pinion with $z = 18$.

5.2 Tooth root fatigue resistance

One of the most important problem in the usage of gears is the teeth fatigue resistance, due to the fact they're subjected to pulsating loads.
In our analysis we used the Lewis method that consider the tooth as a cantilever beam and shear and compressive normal stresses are neglected.
In order to compute the stress state we used the following equation:

$$\sigma_L = \frac{6F_t * h}{b * s_L^2}, \tag{2}$$

where F_t, h, b and s_L are showed in Figure 11a and 11b.
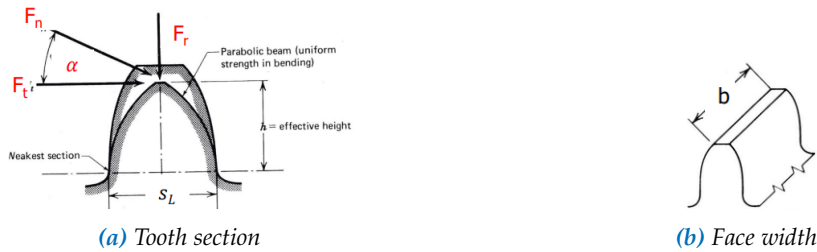

(a) Tooth section

(b) Face width

Figure 11: Tooth details

In our project we used two motors with 10W 50rpm to actuate the machine. From this data we could find the actual force F_t exerted on the teeth:

$$T = \frac{P}{\omega} = \frac{10}{\frac{2\pi 50}{60}} \frac{W}{rad/s} = 1.9 N * m$$

$$F_t = \frac{T}{r} = \frac{1.9}{17.14} \frac{W}{mm} = 111.3 N$$

At this point we can find the stress state, from (2):

$$\sigma_L = \frac{6 * 111.3 * 2.14}{10 * 1.79^2} = 44.6 MPa. \tag{3}$$

The Lewis method provide the nominal stress state at the base of the tooth, in the hypothesis of considering the tooth as a cantilever beam.

All factors affecting the actual value of the stress state should therefore be taken into account in the design. Moreover, the admissible stress must be defined starting from the properties of the material and the production and processing techniques adopted.

A Appendix

A.1 Materials

Table A.1.1: list of available aluminium alloys for T slot profiles with relative mechanical properties (based on ASTM B-221 standard) and extruded profile vendor that provides this results.

ASTM code	$\sigma_{uts}[MPa]$	$\sigma_{ys}[MPa]$	$E[GPa]$	$\nu[\cdot]$	usage	vendors
6005-T5	262	241	70	0.33	profiles	Parker
6105-T5	262	241	70	0.33	profiles	80/20, Parker
6061-T6	262	241	70	0.33	accessories	Parker
6063-T6	206	172	70	0.32	profiles, accessories	Parker
6065-T6	206	172	68	0.32	profiles	tslots

Parameters of the table: σ_{uts} ultimate tensile strength, σ_{ys} yielding strength, E Young's module, ν Poisson's ratio.

σ_{uts} and σ_{ys} are taken directly from the ASTM B-221-05 [**ASTMB221**] standard while other parameters came from T-slot producer's data-sheets [**tslot-ds**] [**parker-ds**] [**8020-ds**].

A.2 Bill of materials

Table A.2.1: *bill of material and estimated costs.*

Code	Product		Quantity	Price
		Manufacturer		
XXX	General piece		1	€—
XXX	General piece		1	€—
		Manufacturer		
XXX	General piece		1	€—
XXX	General piece		1	€—
			Total:	€100.00

INFORMAZIONI SU DOVE SONO STATI PRESI I PREZZI

B Bibliography and references

In order of first appearance: